doi:10.1093/brain/awx120 BRAIN 2017: 140; 2002–2011 | 2002

BRAIN
A JOURNAL OF NEUROLOGY

# Brain inflammation accompanies amyloid in the majority of mild cognitive impairment cases due to Alzheimer's disease

**Peter Parbo,[1] Rola Ismail,[1] Kim V. Hansen,[1] Ali Amidi,[2] Frederik H. Mårup,[1] Hanne Gottrup,[3] Hans Brændgaard,[3] Bengt O. Eriksson,[4] Simon F. Eskildsen,[5] Torben E. Lund,[5] Anna Tietze,[6] Paul Edison,[7] Nicola Pavese,[1,8] Morten G. Stokholm,[1] Per Borghammer,[1] Rainer Hinz,[9] Joel Aanerud[1] and David J. Brooks[1,7,8]**

See Kreisl (doi:10.1093/awx151) for a scientific commentary on this article.

Subjects with mild cognitive impairment associated with cortical amyloid-β have a greatly increased risk of progressing to Alzheimer's disease. We hypothesized that neuroinflammation occurs early in Alzheimer's disease and would be present in most amyloid-positive mild cognitive impairment cases. $^{11}$C-Pittsburgh compound B and $^{11}$C-(R)-PK11195 positron emission tomography was used to determine the amyloid load and detect the extent of neuroinflammation (microglial activation) in 42 mild cognitive impairment cases. Twelve age-matched healthy control subjects had $^{11}$C-Pittsburgh compound B and 10 healthy control subjects had $^{11}$C-(R)-PK11195 positron emission tomography for comparison. Amyloid-positivity was defined as $^{11}$C-Pittsburgh compound B target-to-cerebellar ratio above 1.5 within a composite cortical volume of interest. Supervised cluster analysis was used to generate parametric maps of $^{11}$C-(R)-PK11195 binding potential. Levels of $^{11}$C-(R)-PK11195 binding potential were measured in a selection of cortical volumes of interest and at a voxel level. Twenty-six (62%) of 42 mild cognitive impairment cases showed a raised cortical amyloid load compared to healthy controls. Twenty-two (85%) of the 26 amyloid-positive mild cognitive impairment cases showed clusters of increased cortical microglial activation accompanying the amyloid. There was a positive correlation between levels of amyloid load and $^{11}$C-(R)-PK11195 binding potentials at a voxel level within subregions of frontal, parietal and temporal cortices. $^{11}$C-(R)-PK11195 positron emission tomography reveals increased inflammation in a majority of amyloid positive mild cognitive impairment cases, its cortical distribution overlapping that of amyloid deposition.

1 Department of Nuclear Medicine and PET Centre, Aarhus University Hospital, Aarhus, Denmark
2 Department of Psychology and Behavioural Sciences and Department of Oncology Aarhus University and Aarhus University Hospital, Denmark
3 Department of Neurology, Aarhus University Hospital, Aarhus, Denmark
4 Department of Neurology, Hospitalsenheden Midt, Viborg, Denmark
5 Center of Functionally Integrative Neuroscience (CFIN), Aarhus University, Aarhus, Denmark
6 Institute of Neuroradiology, Charité, Universitätsmedizin, Berlin, Germany
7 Division of Neuroscience, Department of Medicine, Imperial College London, London, UK
8 Division of Neuroscience, Newcastle University, Newcastle, UK
9 Wolfson Molecular Imaging Centre, University of Manchester, Manchester, UK

Correspondence to: Peter Parbo, MD
Department of Nuclear Medicine and PET Centre
Aarhus University Hospital
Nørrebrogade 44, building 10

Received November 4, 2016. Revised April 7, 2017. Accepted April 12, 2017. Advance Access publication May 28, 2017

DK-8000 Aarhus C
Denmark
E-mail: peter.parbo@clin.au.dk

**Keywords:** Alzheimer's disease; mild cognitive impairment; microglial activation; beta-amyloid; positron emission tomography

**Abbreviations:** BPM = biological parametric mapping; MCI = mild cognitive impairment; SPM = statistical parametric mapping

# Introduction

Alzheimer's disease pathology is characterized by abnormal aggregation of the proteins amyloid-β and hyperphosphorylated tau (Braak and Braak, 1991). The amyloid-β fibrils form extracellular beta-sheeted plaques, while hyperphosphorylated tau aggregates intracellularly as neurofibrillary tangles composed of insoluble paired helical filaments (PHF) of tau containing both 3- and 4-tubulin site repeats. In the past decade, PET radiotracers have become available to image *in vivo* aggregated amyloid-β (Klunk *et al.*, 2004) and PHF-tau protein (Chien *et al.*, 2013; Xia *et al.*, 2013). Brain inflammation in the form of microglial activation, its intrinsic immune defence, is also a component of Alzheimer's disease and it has been suggested that it could drive the neurodegenerative processes via cytokine release, which promotes tau hyperphosphorylation (Maphis *et al.*, 2015). However, initially microglial activation may play a protective role in prodromal Alzheimer's disease by clearing amyloid, remodelling connections and releasing growth factors (Hamelin *et al.*, 2016). The exact role of the microglial activation in dementias remains uncertain, as does the timing of its response relative to the deposition of amyloid-β and hyperphosphorylated tau. Activated microglia express translocator protein 18 kDa (TSPO) on the outer membrane of their mitochondria. TSPO has an isoquinoline site that binds $^{11}$C-(R)-PK11195. Varying extents and levels of microglial activation have been reported using TSPO PET imaging in groups of patients with clinically probable Alzheimer's disease and cases with amnestic mild cognitive impairment (MCI) (Stefaniak and O'Brien, 2016). Recent PET studies have reported both raised and absent baseline TSPO binding in MCI cases (Okello *et al.*, 2009; Wiley *et al.*, 2009; Kreisl *et al.*, 2013; Fan *et al.*, 2015; Hamelin *et al.*, 2016). When inflammation is present in Alzheimer's disease, it can be seen in areas with high amyloid-β deposition such as frontal cortex and anterior cingulate, and also in areas with high neurofibrillary tangle density such as medial temporal cortex and hippocampus (Fan *et al.*, 2015).

Subjects with MCI have an increased risk of dementia and the amnestic subtype is most likely to progress to Alzheimer's disease (Petersen, 2004). The presence of biomarkers such as hippocampal atrophy on MRI, low amyloid-$\beta_{42}$ in CSF, and positive amyloid-β PET increases the likelihood that MCI is caused by Alzheimer's pathology (Albert *et al.*, 2011). Identifying early stages of Alzheimer's disease is of interest, as potential disease-modifying drugs are likely to have the greatest impact if administered in the early or preclinical stages of the disease. Anti-inflammatory drugs have been suggested as a way of modifying the progression of Alzheimer's disease (Heneka *et al.*, 2015).

In this study, we hypothesized that amnestic MCI cases with PET evidence of cortical amyloid-β deposition, when compared to MCI cases without raised cortical amyloid-β and healthy control subjects, would show cortical microglial activation detectable with $^{11}$C-(R)-PK11195 PET.

# Materials and methods

## Study subjects

MCI subjects were recruited from Dementia/Memory clinics in Jutland and Funen, Denmark, and by newspaper advertisements. Subjects were included if they presented with a history of declining memory function over a minimum of 6 months, preferably corroborated by an informant and in the absence of a history of recreational drug use, sedative medication, depression, stroke or systemic diseases. Further inclusion criteria were: (i) age 50–85 years; (ii) $\geqslant$7 years of education or good working history; (iii) meets Petersen criteria (Petersen, 2004) for amnestic MCI (no strict memory score cut-off was used); (iv) an informant was available who had frequent contact with the subject and could accompany the subject to clinic visits or be available to talk on the telephone about the subject's memory and complete the interview for Clinical Dementia Rating (CDR); (v) modified Hachinski Ischaemic Scale score $\leqslant$ 4; (vi) Mini-Mental State Examination (MMSE) score 24–30; (vii) Geriatric Depression Scale (GDS-15) score $\leqslant$ 6; and (viii) an MRI examination that excluded MCI arising from structural causes.

Exclusion criteria were: (i) significant neurologic or psychiatric diseases; (ii) history of alcohol and/or recreational drug abuse within 2 years; (iii) contraindications to MRI; (iv) significant reductions in serum B12, red cell folate or thyroid function; and (v) use of medication with known anticholinergic effects (which could impair memory) within the last 3 months or a drug that could impair cognition.

Age-matched healthy control subjects were recruited by newspaper advertisements and screened for neurological diseases. The same inclusion/exclusion criteria as MCI were applied, except that healthy controls had no complaints of memory decline.

The Central Denmark Region Committees on Health Research Ethics approved the study in accordance with the Declaration of Helsinki. All participants signed an informed written consent at enrolment in the study.

## Neuropsychological assessment

Neuropsychological assessments were undertaken in all participants with a test battery comprised of different standardized neuropsychological tests assessing multiple cognitive domains. The assessed cognitive domains and related tests are: (i) processing speed: Coding from Wechsler Adult Intelligence Scale version 4 (WAIS-IV) (Wechsler, 2008), Trail-Making Test Part A (Raitan, 1958) and Stroop Colour and Word Test (Stroop, 1935); (ii) verbal learning and memory: Rey Auditory Verbal Learning Test (Rey, 1964) and Logical Memory I and II from Wechsler Memory Scale (Wechsler, 1989); (iii) working memory: Digit span from WAIS-IV (Wechsler, 2008); (iv) visuospatial abilities: Block design from WAIS-IV (Wechsler, 2008); (v) language function: Controlled Oral Word Association Test (Benton, 1989) and the Boston Naming Test (Kaplan *et al.*, 1983); and (vi) executive functioning: Trail-Making Test Part B (Raitan, 1958) and Stroop Colour and Word test (Stroop, 1935). Trained research assistants undertook all assessments under the supervision of an experienced neuropsychology researcher (A.A.). Normative data were collected from 23 healthy controls of which 15 were from the present study and eight were included from another study under the same research programme. The eight healthy control subjects did not have PK11195 or PiB PET scans, but they were recruited and had neuropsychological assessments identical to the MCI cohort. One of the 15 controls had a few missing test results, hence $n = 22$ in some domain and global scores.

## MRI

MRI was performed on a Skyra 3 T system (Siemens). A MP2RAGE (magnetization prepared rapid gradient-echo with two gradient echo images) (Marques *et al.*, 2010) sequence was used for co-registration of MRI with PET, normalization into standard space, and generation of grey matter masks. MP2RAGE, along with a $T_2$ FLAIR (fluid attenuated inversion recovery) sequence was used to exclude structural lesions, e.g. tumours and territorial infarction. An experienced neuroradiologist (A.T.) visually evaluated all the MRIs.

## Positron emission tomography

All PET scans were acquired on a High Resolution Research Tomograph (ECAT HRRT; CTI/Siemens). A 6-min transmission scan was performed prior to each PET emission scan to enable attenuation correction of emission data. Images were reconstructed with a 3D-OSEM (ordered subset expectation maximum) with 10 iterations and 16 subsets. Point-spread function (PSF) reconstruction was applied to minimize partial volume effects, improve image quality, contrast and quantitative accuracy and achieve a reconstructed resolution of 2.5 mm. Images were not partial volume corrected.

### Amyloid imaging

A mean dose of 391 MBq [standard deviation (SD) = 63] $^{11}$C-PiB (*N*-methyl-[11C]2-(4-methylaminophenyl)-6-hydroxybenzothiazole) was injected intravenously over 10 s, followed by a 10 ml saline flush. Subjects rested for 30 min after injection before installation in scanner. PET was acquired for 50 min in list mode at 40–90 min post-injection. Image data were subsequently rebinned into five frames of 10 min each.

### TSPO imaging

A mean dose of 390 MBq (SD = 47) $^{11}$C-(R)-PK11195 (1-[2-chlorophenyl]-*N*-methyl-*N*-[1-methyl-propyl]-3-isoquinoline carboxamide) (PK11195) was injected intravenously over 10 s, followed by a 10 ml saline flush. Emission scans were initiated with a 30 s 'background' frame before injection of PK11195. The total dynamic scan time was 60.5 min (list mode). Frames were rebinned as: $1 \times 30$ s 'background', $6 \times 10$ s, $2 \times 30$ s, $2 \times 60$ s, $3 \times 120$ s, and $10 \times 300$ s.

## Image analysis

MRI volumes were segmented into grey and white matter images and CSF using MINC software (http://en.wikibooks.org/wiki/MINC). The grey matter masks were convolved with a probabilistic atlas (Hammers *et al.*, 2003) to 'individualize' subject volumes of interest to their grey matter. A weighted average of five bilateral regions (inferiolateral parietal, inferior frontal, middle/inferior temporal, posterior cingulate and parahippocampal cortices) were combined to form a composite volume of interest, used in both PiB and PK11195 analysis. An average grey matter mask from MCI and healthy subjects was used for explicit masking with Statistical Parametric Mapping 8 (SPM8; Wellcome Trust Centre for Neuroimaging).

### $^{11}$C-PiB RATIO images

PiB images of each individual were co-registered to their $T_1$ magnetic resonance images, and then the transformation matrices from the individuals $T_1$ space to MNI space were applied to the PET images using MINC tools. The spatially normalized PiB images were summed from 60–90 min, and voxel signals divided by the mean signal from the individual's cerebellar grey matter volume of interest to generate PiB RATIO images (Edison *et al.*, 2007). Images were not smoothed before extraction of measurements from the composite cortical volume of interest, to minimize spill-in/spill-out. PiB-positivity was defined from the bimodal MCI distribution as a composite cortical PiB RATIO > 1.5. PiB RATIO images were smoothed with a 6 mm full-width at half-maximum (FWHM) Gaussian filter prior to SPM and biological parametric mapping (BPM) analyses.

### PK11195 binding potential maps

After smoothing the dynamic PET images with a 4 mm FWHM 3D Gaussian filter, parametric maps of binding potential ($BP_{ND}$) were generated at a voxel level using the Simplified Reference Tissue Model (SRTM) (Lammertsma and Hume, 1996) implemented in Matlab. As all anatomical regions in the brain can show specific PK11195 binding in Alzheimer's disease, a Supervised Cluster Analysis with 6 classes (Turkheimer *et al.*, 2007) (SVCA6) was used to localize a cluster of voxels from the dynamic images of each MCI case, which provided a reference tissue input function representing normal grey matter kinetics. The PK11195 images were spatially normalized into MNI space in the same manner as described for the PiB images. PK11195 images were smoothed with a 6 mm FWHM Gaussian filter prior to SPM and BPM analyses. Levels of PK11195 $BP_{ND}$ are sampled from 13 volumes of interest, comprising left and right volumes of interest of six cortical regions (frontal, lateral parietal, lateral

temporal, medial temporal, precuneus and posterior cingulate) and the composite volume of interest.

### Statistical parametric mapping and biological parametric mapping

Clusters of increased PK11195 binding are scattered and so a volume of interest approach based on Brodmann regions of the brain will include both voxels with raised and normal PK11195 signal. Alongside a predefined volume of interest approach, parametric maps of PK11195 $BP_{ND}$ were interrogated with SPM to detect clusters of voxels with significantly increased PK11195 $BP_{ND}$ in the PiB-positive MCI group compared to the healthy controls group. The amplitude of increased microglial activation in these clusters of increased PK11195 $BP_{ND}$ was then quantified, thus avoiding dilution by partial volume effects from surrounding normal voxels—a problem with anatomically based volumes of interest. SPMs comparing PiB-positive MCI > healthy controls, PiB-positive > PiB-negative MCI, and PiB-negative MCI ≠ healthy controls were generated within a mask defined by the voxels where an ANOVA (uncorrected $P < 0.001$) showed a significant mean difference between these three groups (Friston *et al.*, 2006). This map was subsequently thresholded at $P < 0.001$ to identify the cluster size corresponding to an FWE corrected cluster level $P$-value < 0.05. This cluster extent was then used as a threshold to construct the final SPMs.

BPM (Casanova *et al.*, 2007) (BPM toolbox running in SPM5) was used to detect voxels where there was a positive correlation between individual z-scores of PiB RATIO and PK11195 $BP_{ND}$ in PiB-positive MCI cases. The z-score maps were generated for each PiB-positive MCI case using mean and SD values from PiB RATIO and PK11195 $BP_{ND}$ maps of healthy controls (PiB $n = 10$ healthy controls, PK11195 $n = 10$ healthy controls).

## Statistical analysis

Data were analysed using STATA version 13.1 (StataCorp LP, Texas, USA) and SPSS22 (SPSS Inc., Chicago, Illinois). Differences in non-imaging variables between groups were assessed using ANOVA with *post hoc* pairwise mean comparisons (Bonferroni corrected) for normally distributed continuous data, Pearson's $\chi^2$ tests for categorical variables, and Kruskal-Wallis with *post hoc* Wilcoxon rank-sum tests (Bonferroni corrected) for skewed ordinal variables. $P$-values < 0.05 were considered statistically significant. Levels of PK11195 BP were analysed using a repeated measures two-way ANOVA model with three groups (PiB-positive MCI, PIB-negative MCI, control group) and 13 volumes of interest as inner subject factors. For the neuropsychological data test-specific z-scores were calculated using test scores from the healthy control group. Domain-specific z-scores were then calculated as the mean of all domain-relevant tests. Between-group differences in the domain-specific z-scores were tested using ANCOVA adjusted for age.

# Results

The MCI cohort comprised 42 subjects (mean age 70 years; range 50–83) who had both PiB and PK11195 PET. Fifteen healthy control subjects were included in this PET study (mean age 68 years; range 58–80 years), of which 12 healthy controls had PiB PET and 10 healthy controls had PK11195 PET. Seven of the 15 healthy controls had both PiB and PK11195 PET, while the rest had either PiB or PK11195 PET only (see Tables 1 and 2 for further details). The majority of the MCI subjects had their PiB and PK11195 PET scans acquired on the same day. In some cases a tracer production failed and had to be rescheduled. The interval between PIB and PK11195 PET was less than 5 weeks within those MCIs having to return for a rescheduled PET scan. In MCI and controls, the intervals between PET and MRI, and PET and neuropsychological testing were less than 10 and 8 weeks, respectively, with a single control outlier having more than 10 weeks between assessments.

Twenty-six (62%) of the 42 MCI cases had a composite cortical PiB RATIO > 1.5 and were categorized as PiB-positive. Two (17%) of the 12 control subjects were also PiB-positive (Fig. 1) and so represented outliers.

The estimated means of PK11195 $BP_{ND}$ for volumes of interest are shown in Fig. 2 with respective 95% confidence intervals. Repeated measures ANOVA revealed a significant group effect [$F(2,49) = 7.22$, $P = 0.0018$], whereas regional PK11195 binding did not differ between groups as indicated by non-significant interaction term. *Post hoc* group comparisons showed elevated PK11195 binding in the PIB-positive group versus controls ($P = 0.02$) and PIB-negative subjects ($P < 0.001$). PIB-negative subjects had no difference of PK11195 binding compared to healthy control subjects ($P = 0.4$). Adjusting for age differences did not change the results.

To estimate the amplitude of focal PK11195 $BP_{ND}$ rises in PiB-positive MCI cases, we measured the PK11195 $BP_{ND}$ within the clusters of voxels of raised $BP_{ND}$ (in total 3652 voxels) localized by SPM when interrogating the 26 PiB-positive MCI cases versus 10 healthy controls. SPM identified clusters of significantly raised PK11195 $BP_{ND}$ in PiB-positive MCI individuals targeting the lateral temporal and, to a lesser extent, frontal and parietal areas (Fig. 3A and B). There is a trend towards a left lateralization in Fig. 3A but this is not evident in Fig. 3B, and not reflected in either the volume of interest results in Fig. 2 or in the neuropsychological findings (Table 2), hence we do not feel to have demonstrated clear-cut lateralization.

PiB-positive MCIs showed a mean PK11195 $BP_{ND}$ of 0.15 [range (0.026–0.39)] within the identified clusters, while controls had a mean of−0.029 [range (−0.088–0.069)]. Twenty-two (85%) of the PiB-positive MCI cases had PK11195 binding above the range of controls whereas only four (25%) of the PiB-negative MCI had raised PK11195 binding within the same voxels and this was borderline (Fig. 4). Excluding the two PiB-positive controls from the SPM analysis did not significantly change our findings. Healthy controls did not show any clusters with higher PK11195 binding when running the opposite SPM analysis, PiB-positive < healthy controls. An additional

**Table 1 Participant characterization**

| | PiB + MCI ($n$ = 26) | PiB − MCI ($n$ = 16) | Healthy controls ($n$ = 15) | $P$-value |
|---|---|---|---|---|
| Age, years, mean ± SD [range] | 73.3 ± 6.2 [62–83] | 65.8 ± 8.4 [50–79] | 68.3 ± 6.6 [58–80] | 0.003[a] |
| Gender, males, $n$ (%) | 17 (65) | 7 (44) | 6 (40) | 0.2 |
| Education, years, median | 12 | 11.5 | 13 | 0.2 |
| Subjects using NSAID, $n$ (%) | 9 (35) | 4 (25) | 1 (7) | 0.1 |
| MMSE score, median [range] | 27 [23–30] | 28 [23–30] | 29 [25–30] | 0.005[b] |
| CDR sum of boxes, median | 1.5 | 1 | 0 | 0.0001[b,c] |
| Geriatric Depression Scale, mean ± SD | 1.7 ± 1.8 | 1.1 ± 1.0 | 0.4 ± 0.7 | 0.02[b] |
| PiB dose, MBq, mean ± SD ($n$) | 365 ± 79 | 409 ± 25 | 422 ± 28 (12) | 0.01[b] |
| PK11195 dose, MBq, mean ± SD ($n$) | 384 ± 47 | 375 ± 57 | 389 ± 21 (10) | 0.9 |
| Subjects with Fazekas score 0 / 1 / 2 / 3, $n$ | 4 / 10 / 9 / 2 | 5 / 6 / 4 / 1 | 7 / 6 / 1 / 0 | 0.26 |

Data are presented as mean ± SD, number of subjects (%) or medians. Differences between groups are tested (using ANOVA, Pearson's $\chi^2$ or Kruskal-Wallis), and resulting $P$-values are presented in the rightmost column. One PiB + MCI and one control subject did not have $T_2$ FLAIR, hence missing Fazekas scores. *Post hoc* pairwise group comparisons (Bonferroni corrected).

[a]$P < 0.05$ for PiB + MCI versus PiB − MCI.

[b]$P < 0.05$ for PiB + MCI versus controls.

[c]$P < 0.05$ for PiB − MCI versus controls.

CDR = Clinical dementia rating; MMSE = Mini-Mental State Examination; NSAID = non-steroidal anti-inflammatory drug; PiB + = PiB-positive MCI; PiB − = PiB-negative MCI.

**Table 2 Neuropsychological testing**

| | PiB + MCI ($n$ = 26) | PiB − MCI ($n$ = 16) | Controls | $P$-value (ANCOVA) |
|---|---|---|---|---|
| Processing speed, mean z-score ± SD | −1.5 ± 0.8 | −0.7 ± 1.1 | 0.0 ± 0.7 ($n$ = 22) | <0.0001[a,c] |
| Working memory, mean z-score ± SD | −0.6 ± 1.0 | −0.2 ± 1.4 | 0.0 ± 1.0 ($n$ = 23) | 0.4 |
| Visuospatial function, mean z-score ± SD | −0.9 ± 1.9 | − 0.2 ± 1.7 | 0.0 ± 1.0 ($n$ = 23) | 0.5 |
| Global memory, mean z-score ± SD | −1.5 ± 1.0 | −0.5 ± 1.2 | 0.0 ± 0.6 ($n$ = 22) | <0.0001[a] |
| Language, mean z-score ± SD | − 0.9 ± 1.1 | −0.8 ± 1.7 | 0.0 ± 0.9 ($n$ = 22) | 0.06 |
| Executive function, mean z-score ± SD | −1.2 ± 0.9 | −0.4 ± 1.3 | 0.0 ± 0.7 ($n$ = 22) | 0.004[a] |
| Global composite score, mean z-score ± SD | −1.2 ± 0.8 | −0.4 ± 1.1 | 0.0 ± 0.3 ($n$ = 22) | <0.0001[a] |

Differences in neuropsychological domain and global mean z-scores assessed with age-adjusted ANCOVA across the three groups (PiB + MCI, PiB − MCI and healthy controls) and presented with $P$-values. Mean z-scores are by definition zero for the healthy controls. *Post hoc* pairwise group comparisons (Bonferroni corrected).

[a]$P < 0.05$ for PiB + MCI versus controls.

[b]$P < 0.05$ for PiB − MCI versis controls.

small cluster of raised $^{11}$C-PK11195 binding was detected in the left hippocampus when PIB-positive MCI were compared with PIB-negative MCI cases, but not when PIB-positive MCI were compared with healthy control subjects (Fig. 3D and E).

Because of differences in mean age between the PiB-positive and PiB–negative MCI group, ANCOVA was performed to extract the variance in PK11195 $BP_{ND}$ at a voxel level arising due to these factors. The age corrected SPMs and uncorrected SPMs showed similar distributions of voxels with significantly raised PK11195 $BP_{ND}$ for the PiB-positive MCI cases.

BPM was used to localize voxels where individual levels of PiB RATIO and PK11195 $BP_{ND}$ had a positive correlation in the group of 26 PiB-positive MCI cases. This approach detected clusters of positive correlation in subregions of frontal, temporal and parietal cortices (Fig. 5A), which differed from the areas of raised PK11195 binding identified in PiB-positive MCI with SPM (Fig. 3A and B).

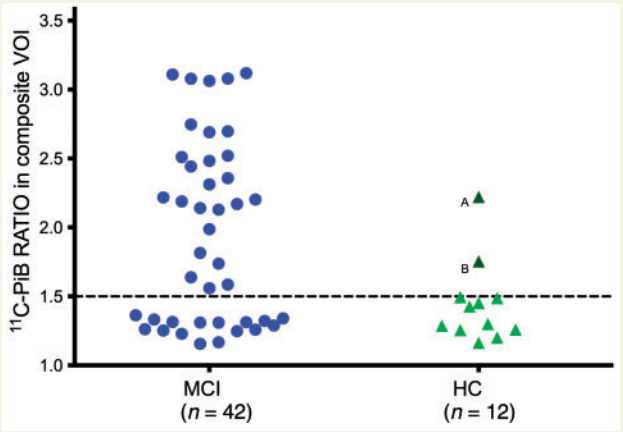


**Figure 1 Scatterplot of 11C-PiB RATIO in composite cortical volume of interest.** Twenty-six (62%) of MCI cases were above the 1.5 cut-off line, and hence classified as PiB-positive MCI. The two PiB-positive healthy controls (HC) are marked with the letters 'A' and 'B' for identification in Fig. 4. VOI = volume of interest.

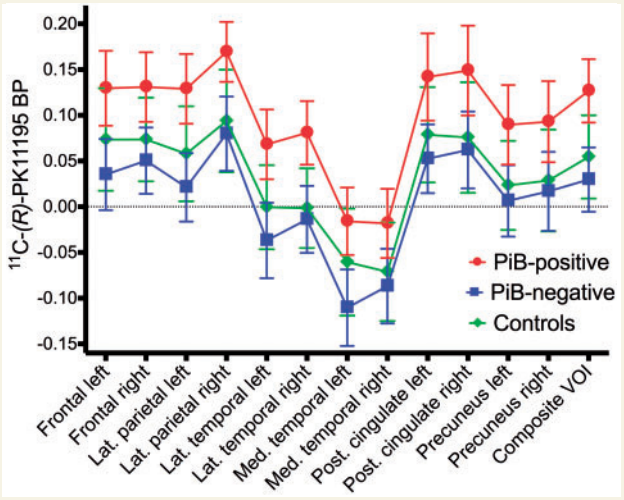


**Figure 2 Regional PK11195 $BP_{ND}$ in PiB-positive MCI, PiB-negative MCI and healthy controls.** Means and 95% confidence intervals of PK11195 $BP_{ND}$ in left and right frontal, lateral parietal, lateral and medial temporal, precuneus and posterior cingulate cortical volumes of interest, and the composite volume of interest. Repeated measures ANOVA revealed a significant group effect [$F(2,49) = 7.22$, $P = 0.0018$]. *Post hoc* group comparisons showed elevated PK11195 binding in the PIB-positive group compared to controls ($P = 0.02$) and PIB-negative subjects ($P < 0.001$). VOI = volume of interest.

# Discussion

This study provides evidence that neuroinflammation is a component of the neurodegenerative pathology present in a majority of amyloid-β positive MCI; these are the cases who are most likely to progress to Alzheimer's dementia. We detected clusters of raised microglial activation in two-thirds of our PiB-positive MCI cases compared to controls. However, other studies have failed to detect evidence of microglial activation in MCI (Wiley *et al.*, 2009; Kreisl *et al.*, 2013). While Wiley *et al.* supported the viewpoint that microglia activation is likely to be an early feature in Alzheimer's disease, they concluded that their $^{11}$C-(R)-PK11195 PET study lacked the sensitivity to detect it. Our ability to demonstrate a high prevalence of microglial activation in prodromal Alzheimer's disease could reflect the combined use of a high sensitivity HRRT scanner, a more sensitive SVCA6 kinetic modelling approach, and a larger sample size than previous works.

Four (15%) of our PiB-positive MCI subjects had PK11195 $BP_{ND}$ values still within the upper normal range. It is, therefore, possible to have amyloid deposition without significant neuroinflammation being present and these MCI cases may prove to progress less rapidly in the future than those with both amyloid plaques and microglial activation evident on PET scanning. However, the opposite situation could be that activated microglia may play a protective role in early Alzheimer's disease as suggested by Hamelin *et al.* (2016). The baseline scans of our cases will represent different time points of their disease trajectory and, if inflammation declines as MCI progresses—as suggested in a recent review (Calsolaro and Edison, 2016) and by findings from a recent longitudinal study using $^{18}$F-DPA714 PET (Hamelin *et al.*, 2016), this could also account for negative findings in some of our cases. We propose to follow our MCI cohort for a minimum of 2 years and rescan them to determine their trajectory of inflammation.

The majority of PiB-negative MCI cases had PK11195 $BP_{ND}$ values within the range of controls. It remains unclear whether such cases have neurodegenerative pathology and will progress to dementia on follow-up. PiB-negative MCI cases represent a heterogeneous group and their memory problems can arise from non-Alzheimer pathologies such as frontotemporal dementia or vascular disease or non-degenerative conditions such as stress, depression, or sleep deprivation, though we have tried to exclude these conditions. Interestingly, two of our normal controls were PiB-positive outliers and they showed no evidence of raised microglial activation. This would favour inflammation arising as a secondary event to amyloid-β aggregation.

$^{11}$C-PK11195 PET was chosen for *in vivo* identification of microglial activation in neurodegenerative diseases because of the long experience and substantial literature existing on its successful use and reproducible findings in Alzheimer's (Cagnin *et al.*, 2001), Parkinson's (Gerhard *et al.*, 2006) and Huntington's disease (Pavese *et al.*, 2006). Additionally, the PK11195 tracer is not significantly influenced by the *TSPO* polymorphism expressed by cases. Finally we have long in-house experience with production of $^{11}$C-PK11195. A limitation is the relatively lower signal-to-noise ratio of PK11195 tracer compared to newer tracers. The lower signal-to-noise ratio can make it difficult to

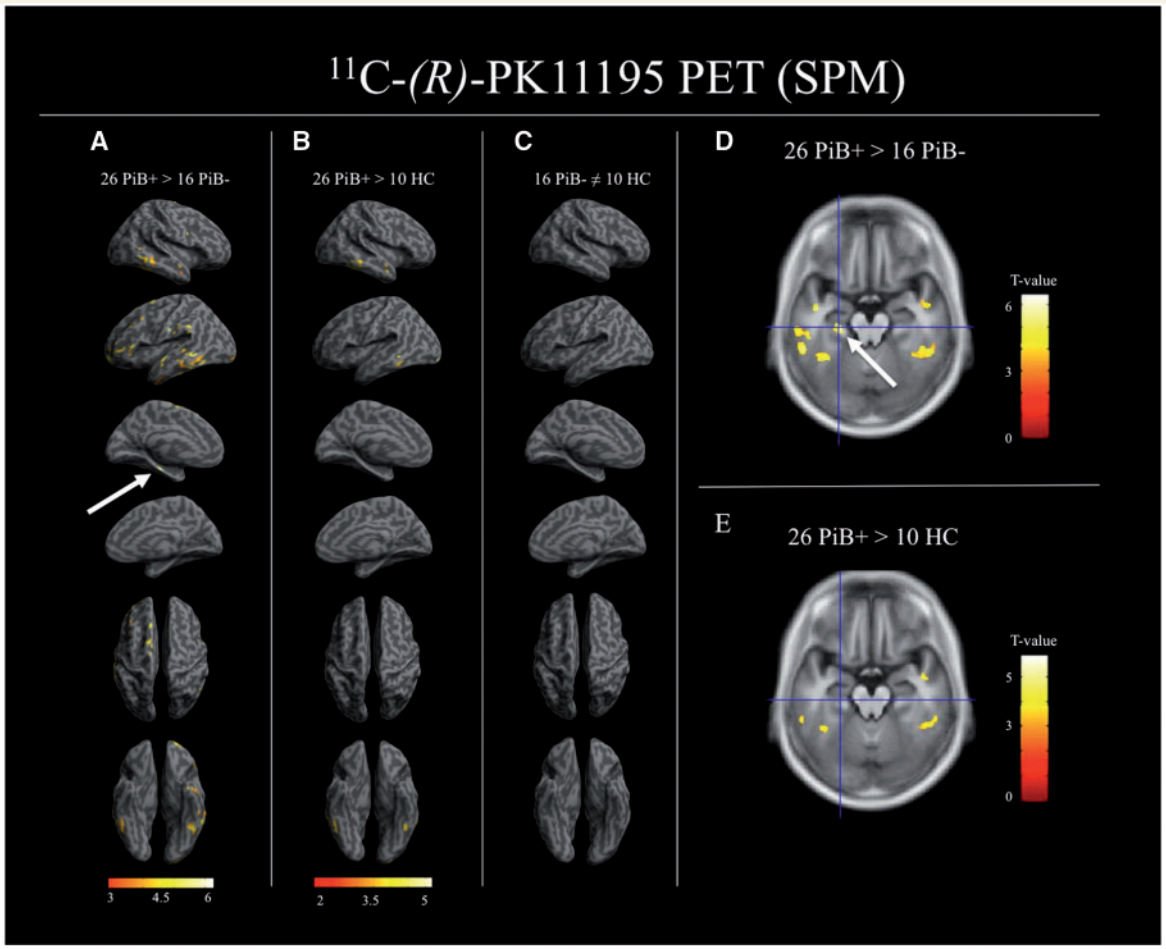


**Figure 3 Results from SPM analyses of group comparisons of PK11195 $BP_{ND}$ maps.** (**A–C**) Two-sample *t*-tests between PiB-positive and PiB-negative MCI, PiB-positive MCI and healthy controls (HC), and between PiB-negative MCI and healthy controls. (**D** and **E**) PiB + MCI > PiB − MCI reveals a cluster in the left hippocampus (marked with a white arrow in Fig. 3A and D). This hippocampal cluster is not seen in the PiB + MCI > HC comparison (Fig. 3E, cross hair positioned in same coordinate as in Fig. 3D). All comparisons are processed within a mask defined by a voxel-wise ANOVA, and the displayed clusters are of significant size (FWE cluster-level $P < 0.05$, with a cluster-defining threshold of $P < 0.001$).

find small group differences, and we can potentially have missed small changes in some regions. Another possible limitation to the study is our relatively small groups of healthy controls for PK11195 and PiB PET.

BPM localized brain clusters where there were significant correlations between levels of amyloid and levels of inflammation (Fig. 5). These clusters differed from those with raised inflammation detected by a between group SPM analysis comparing PiB-positive MCI cases with controls (Fig. 3). This is because BPM identifies voxels where inflammation and amyloid levels are correlated as opposed to voxels where there is a mean increase in inflammation due to any cause. As illustrated in Fig. 5B and C, positive correlation between PiB SUVR and PK11195 $BP_{ND}$ can be identified in some brain regions. However, the mean PK11195 binding in these specific clusters is not significantly increased compared to control subjects, therefore the clusters identified by BPM correlation analysis will not necessarily match those found in a SPM analysis comparing the mean binding in the two groups. The BPM findings link amyloid deposition and inflammation, particularly in posterior brain regions. However, we cannot exclude that other pathologies may be influencing inflammation with a different distribution to amyloid, such as neurofibrillary tau tangles, for example.

The conservative PiB RATIO cut-off at 1.5 was defined from the bimodal distribution of PiB uptake in our MCI cases and chosen to ensure that the prodromal Alzheimer's disease group we identified had a significant level of cortical amyloid. Additionally, the use of a HRRT scanner provides images with higher sensitivity than the conventional PET-CT cameras usually used for PiB PET. Use of the HRRT may also provide a greater specific cortical signal due to reduced spill-in to cerebellar grey matter, resulting in higher ratios measured within cerebral cortical regions.

The neuropsychological test results indicated that PiB-positive MCI cases performed significantly worse in the

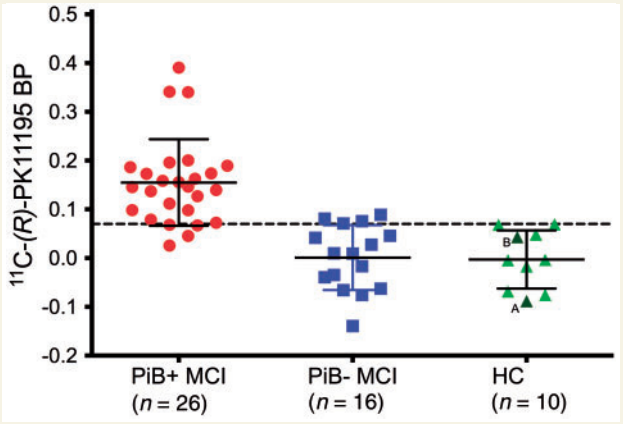


**Figure 4 Scatterplot of individual PK11195 $BP_{ND}$ across clusters localized by the SPM.** Individual PK11195 $BP_{ND}$ levels averaged across all voxels contained in the clusters localized by the SPM comparing PiB-positive MCI with healthy controls (HC) (Fig. 3B). Twenty-two (85%) of the 26 PiB-positive MCI cases showed PK11195 binding levels above the healthy control range. PK11195 BPND levels for individual PiB-negative MCI and healthy control subjects averaged across voxels at the same locations are also shown in the plot. Letters 'A' and 'B' indicate the two PiB-positive controls seen in Fig. 1. The dashed horizontal line at $y = 0.07$ marks the upper limit of the healthy control range; short solid lines are group means ± 1 SD.

memory domain compared with the PiB-negative MCI cases and healthy controls. Moreover, the testing also indicated that the MCI cohort was clinically heterogeneous in terms of affected domains (Table 2 and Supplementary Fig. 1), which could have increased variance in the size and extent of the regional cerebral PK11195 binding.

In summary, this study provides supportive evidence that neuroinflammation is a component of the neurodegenerative pathology in a majority of MCI cases due to Alzheimer's disease. Statistical parametric mapping localized clusters of raised PK11195 binding in 85% of our amyloid-β-positive amnestic MCI (prodromal Alzheimer's disease) subjects. We found raised inflammation in only 25% of the amyloid-β-negative MCI subjects and this was borderline. The distribution of neuroinflammation in amyloid-β-positive MCI mirrored the distribution of the amyloid-β in the frontal, temporal and parietal cortices. However, the temporal order of these pathologies still needs to be investigated further and will probably require longitudinal PET studies of high-risk normal subjects. Our MCI cohort will be followed for a minimum of 2 years and rescanned to determine whether neuroinflammation declines or increases with progression towards Alzheimer's disease. On occasion raised amyloid-β can be detected in

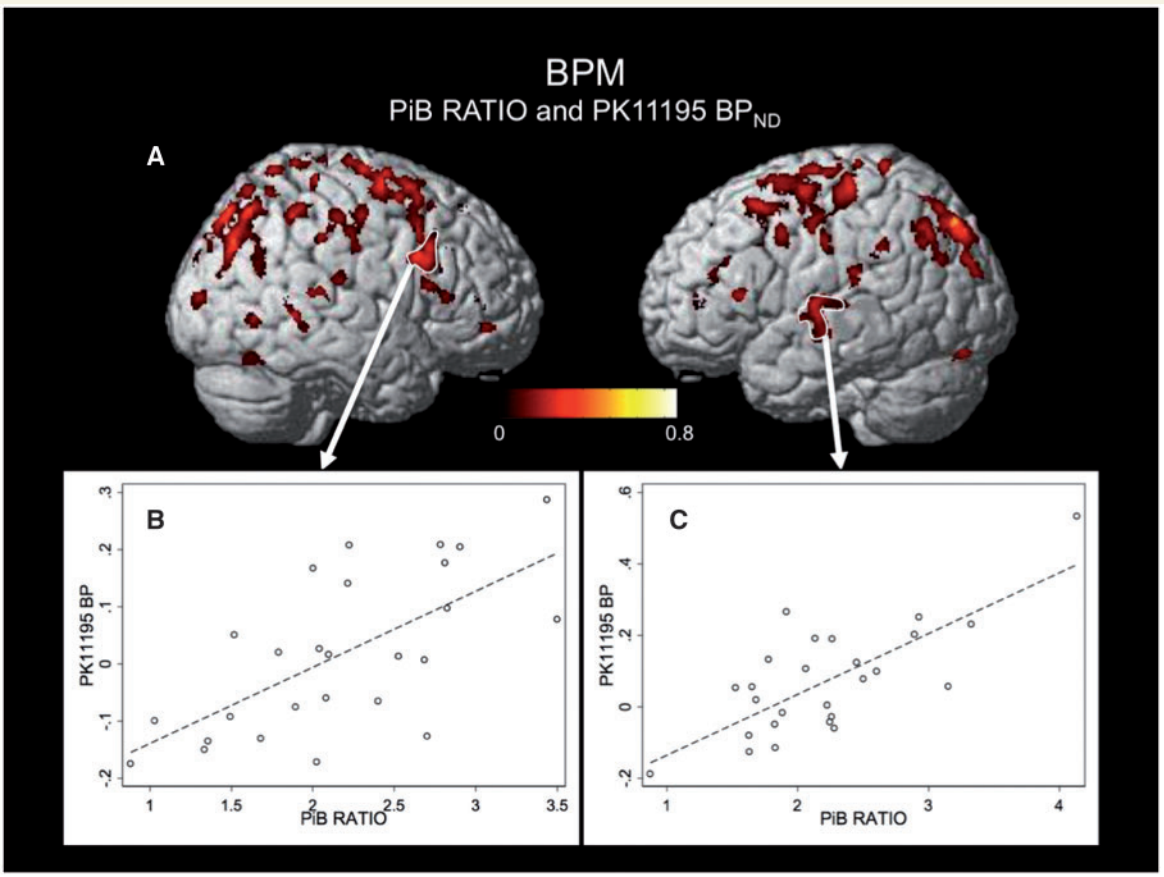


**Figure 5 BPM of PiB RATIO and PK11195 $BP_{ND}$.** (**A**) Clusters of voxels with a positive correlation between PiB RATIO and PK11195 BPND within 26 PiB-positive MCI cases. Voxel-level uncorrected $P < 0.001$, cluster-level corrected at $P < 0.05$. (**B** and **C**) Two clusters are picked for extraction of individual measures of the 26 PiB-positive MCI cases (**B**, right inferior frontal gyrus; **C**, left superior temporal gyrus).

MCI and normal subjects without evidence of neuroinflammation. Follow-up of such subjects may determine whether they have a more benign syndrome than the MCI subjects who have both amyloid-β deposition and neuroinflammation present.

## Acknowledgements

We thank Anne Sofie Møller Andersen for great administrative support, consultants Petya Hykkelsbjerg and Lene Wermuth for referring subjects with MCI, Arne Møller for help with PET scans and Zhen Fan for assistance getting started with BPM.

## Funding

The study was financially supported by a grant from the Danish Council for Independent Research and the Lundbeck Foundation. P.P. and R.I. were funded by The Danish Council for Independent Research. P.E. was funded by the Medical Research Council and now by Higher Education Funding Council for England (HEFCE). He has also received grants from Alzheimer's Research, UK, Alzheimer's Drug Discovery Foundation, Alzheimer's Society, UK, Novo Nordisk, Piramal Life Science and GE Healthcare. R.H. received funding from the European Union's Seventh Framework Programme (FP7/2007-2013) under grant agreement no HEALTH-F2-2011-278850 Imaging of Neuroinflammation in Neurodegenerative Diseases (INMiND). D.J.B. has received research grants and non-financial support from the Medical Research Council, grants from The Danish Council for Independent Research, grants from The Lundbeck Foundation, grants from Alzheimer's Research Trust, grants from Michael J Fox foundation and grants from the European Commission; GE Healthcare consultancy.

## Supplementary material

Supplementary material is available at *Brain* online.

## References

Albert MS, DeKosky ST, Dickson D, Dubois B, Feldman HH, Fox NC, et al. The diagnosis of mild cognitive impairment due to Alzheimer's disease: recommendations from the National Institute on Aging-Alzheimer's Association workgroups on diagnostic guidelines for Alzheimer's disease. Alzheimers Dement 2011; 7: 270–9.

Benton A. Multilingual Aphasia examination. Iowa City: AJA Associates; 1989.

Braak H, Braak E. Neuropathological stageing of Alzheimer-related changes. Acta Neuropathol 1991; 82: 239–59.

Cagnin A, Brooks DJ, Kennedy AM, Gunn RN, Myers R, Turkheimer FE, et al. *In-vivo* measurement of activated microglia in dementia. Lancet 2001; 358: 461–7.

Calsolaro V, Edison P. Neuroinflammation in Alzheimer's disease: current evidence and future directions. Alzheimers Dement 2016; 12: 719–32.

Casanova R, Srikanth R, Baer A, Laurienti PJ, Burdette JH, Hayasaka S, et al. Biological parametric mapping: a statistical toolbox for multimodality brain image analysis. Neuroimage 2007; 34: 137–43.

Chien DT, Bahri S, Szardenings AK, Walsh JC, Mu F, Su MY, et al. Early clinical PET imaging results with the novel PHF-tau radioligand [F-18]-T807. J Alzheimers Dis 2013; 34: 457–68.

Edison P, Archer H, Hinz R, Hammers A, Tai Y, Hotton G, et al. Amyloid, hypometabolism, and cognition in Alzheimer disease: an [11C]PIB and [18F]FDG PET study. Neurology 2007; 68: 501–8.

Fan Z, Aman Y, Ahmed I, Chetelat G, Landeau B, Ray Chaudhuri K, et al. Influence of microglial activation on neuronal function in Alzheimer's and Parkinson's disease dementia. Alzheimers Dement 2015; 11: 608–21.e7.

Friston KJ, Rotshtein P, Geng JJ, Sterzer P, Henson RN. A critique of functional localisers. Neuroimage 2006; 30: 1077–87.

Gerhard A, Pavese N, Hotton G, Turkheimer F, Es M, Hammers A, et al. *In vivo* imaging of microglial activation with [11C](R)-PK11195 PET in idiopathic Parkinson's disease. Neurobiol Dis 2006; 21: 404–12.

Hamelin L, Lagarde J, Dorothé G, Leroy C, Labit M, Comley RA, et al. Early and protective microglial activation in Alzheimer's disease: a prospective study using 18 F-DPA-714 PET imaging. Brain 2016: 1252–64.

Hammers A, Allom R, Koepp MJ, Free SL, Myers R, Lemieux L, et al. Three-dimensional maximum probability atlas of the human brain, with particular reference to the temporal lobe. Hum Brain Mapp 2003; 19: 224–47.

Heneka MT, Carson MJ, El Khoury J, Landreth GE, Brosseron F, Feinstein DL, et al. Neuroinflammation in Alzheimer's disease. Lancet Neurol 2015; 14: 388–405.

Kaplan E, Goodglass H, Weintraub S. The Boston naming test. Philadelphia: Lea & Febiger; 1983.

Klunk W, Engler H, Nordberg A, Wang Y, Blomqvist G, Holt DP, et al. Imaging brain amyloid in Alzheimer's disease with Pittsburgh compound-B. Ann Neurol 2004; 55: 306–19.

Kreisl WC, Lyoo CH, McGewier M, Snow J, Jenko KJ, Kimora N, et al. *In vivo* radioligand binding to translocator protein correlates with severity of Alzheimer's disease. Brain 2013; 136: 2228–38.

Lammertsma AA, Hume SP. Simplified reference tissue model for PET receptor studies. Neuroimage 1996; 158: 153–8.

Maphis N, Xu G, Kokiko-Cochran ON, Jiang S, Cardona A, Ransohoff RM, et al. Reactive microglia drive tau pathology and contribute to the spreading of pathological tau in the brain. Brain 2015; 138: 1738–55.

Marques JP, Kober T, Krueger G, van der Zwaag W, Van de Moortele PF, Gruetter R. MP2RAGE, a self bias-field corrected sequence for improved segmentation and T1-mapping at high field. Neuroimage 2010; 49: 1271–81.

Okello A, Edison P, Archer HA, Turkheimer FE, Kennedy J, Bullock R, et al. Microglial activation and amyloid deposition in mild cognitive impairment. A PET study. Neurology 2009; 72: 56–62.

Pavese N, Gerhard A, Tai YF, Ho AK, Turkheimer F, Barker RA, et al. Microglial activation correlates with severity in Huntington disease: a clinical and PET study. Neurology 2006; 66: 1638–43.

Petersen RC. Mild cognitive impairment as a diagnostic entity. J Intern Med 2004; 256: 183–94.

Raitan R. Validity of the trail making test as an indicator of organic brain damage. Percept Mot Ski 1958; 8: 271–6.

Rey A. L'examen clinique en psychologie. France: Universitaires de France; 1964.

Stefaniak J, O'Brien J. Imaging of neuroinflammation in dementia: a review. J Neurol Neurosurg Psychiatry 2016; 87: 21–28.

Stroop J. Studies of interference in serial verbal reactions. J Exp Psychol 1935; 18: 643–62.

Turkheimer FE, Edison P, Pavese N, Roncaroli F, Anderson AN, Hammers A, et al. Reference and target region modeling of 11C-(R)-PK11195 brain studies. J Nucl Med 2007; 48: 158–67.

Wechsler D. Wechsler memory scale. 3rd edn. San Antonio, TX: Pearson; 1989.

Wechsler D. Wechsler adult intelligence scale. 4th edn. San Antonio, TX: Pearson; 2008.

Wiley CA, Lopresti BJ, Venneti S, Price J, Klunk WE, DeKosky ST, et al. Carbon 11-labeled Pittsburgh compound B and carbon 11-labeled (R)-PK11195 positron emission tomographic imaging in Alzheimer disease. Arch Neurol 2009; 66: 60–7.

Xia CF, Arteaga J, Chen G, Gangadharmath U, Gomez LF, Kasi D, et al. [(18)F]T807, a novel tau positron emission tomography imaging agent for Alzheimer's disease. Alzheimers Dement 2013; 9: 666–76.